AFRL-RY-WP-TR-2011-1304

EPITAXIAL HYBRID SILICON TECHNOLOGY

J.E. Bowers, Christopher Palmstrom, Philip A. Mages, Brian D. Schultz, and M.J.R. Heck

University of California, Santa Barbara

AUGUST 2011
Final Report

Approved for public release; distribution unlimited.

See additional restrictions described on inside pages

STINFO COPY

AIR FORCE RESEARCH LABORATORY
SENSORS DIRECTORATE
WRIGHT-PATTERSON AIR FORCE BASE, OH 45433-7320
AIR FORCE MATERIEL COMMAND
UNITED STATES AIR FORCE

NOTICE AND SIGNATURE PAGE

Using Government drawings, specifications, or other data included in this document for any purpose other than Government procurement does not in any way obligate the U.S. Government. The fact that the Government formulated or supplied the drawings, specifications, or other data does not license the holder or any other person or corporation; or convey any rights or permission to manufacture, use, or sell any patented invention that may relate to them.

This report was cleared for public release by the USAF 88th Air Base Wing (88 ABW) Public Affairs (AFRL/PA) Office and is available to the general public, including foreign nationals. Copies may be obtained from the Defense Technical Information Center (DTIC) (http://www.dtic.mil).

AFRL-RY-WP-TR-2011-1304 HAS BEEN REVIEWED AND IS APPROVED FOR PUBLICATION IN ACCORDANCE WITH THE ASSIGNED DISTRIBUTION STATEMENT.

*//Signature//

VASSILIOS KOVANIS, Project Engineer
Electro-Optic Components Branch
Aerospace Components Division

//Signature//

ATILLA SZEP, Acting Chief
Electro-Optic Components Branch
Aerospace Components Division

//Signature//

JAMES LOUTHAIN, Lt Col, USAF
Aerospace Components Division
Sensors Directorate

This report is published in the interest of scientific and technical information exchange, and its publication does not constitute the Government's approval or disapproval of its ideas or findings.

*Disseminated copies will show "//Signature//" stamped or typed above the signature blocks.

REPORT DOCUMENTATION PAGE

Form Approved
OMB No. 0704-0188

1. REPORT DATE *(DD-MM-YY)*	2. REPORT TYPE	3. DATES COVERED *(From - To)*
August 2011	Final	30 March 2010 – 30 June 2011

4. TITLE AND SUBTITLE
EPITAXIAL HYBRID SILICON TECHNOLOGY

5a. CONTRACT NUMBER
FA8650-10-1-7031

5b. GRANT NUMBER

5c. PROGRAM ELEMENT NUMBER
62716E

6. AUTHOR(S)
J.E. Bowers, Christopher Palmstrom, Philip A. Mages, Brian D. Schultz, and M.J.R. Heck

5d. PROJECT NUMBER
ARPR

5e. TASK NUMBER
YD

5f. WORK UNIT NUMBER
ARPRYD2X

7. PERFORMING ORGANIZATION NAME(S) AND ADDRESS(ES)
University of California, Santa Barbara
3227 Cheadle Hall
Santa Barbara CA 93106-0001

8. PERFORMING ORGANIZATION REPORT NUMBER

9. SPONSORING/MONITORING AGENCY NAME(S) AND ADDRESS(ES)
Air Force Research Laboratory
Sensors Directorate
Wright-Patterson Air Force Base, OH 45433-7320
Air Force Materiel Command
United States Air Force

Defense Advanced Research Projects Agency/ (DARPA)
3701 N. Fairfax Drive
Arlington, VA 22203-1714

10. SPONSORING/MONITORING AGENCY ACRONYM(S)
AFRL/RYDP

11. SPONSORING/MONITORING AGENCY REPORT NUMBER(S)
AFRL-RY-WP-TR-2011-1304

12. DISTRIBUTION/AVAILABILITY STATEMENT
Approved for public release; distribution unlimited.

13. SUPPLEMENTARY NOTES
Report contains color. PA Case Number: 88ABW2011-5631; Clearance Date: 20 Oct 2011.

14. ABSTRACT
We have investigated a wide range of conditions for MOCVD epitaxial layer overgrowth, and studies the impact on coalescence on the ELO patterns and orientations. We have found conditions that allow us to grow such that the coalesced regions are defect free. This is a first for MOCVD and it is the first for growth across a significantly wide field. The fundamental nucleation and growth of As and Sb based III-V semiconductors on SiO2 masked Si(100) and InP(100) surfaces were investigated via molecular beam epitaxy (MBE) to determine the best growth windows for nucleation and lateral overgrowth. Antimonides provide better lateral overgrowth than arsenides indicating transitions from layer-by-layer to step flow growth regimes in MBE may be critical for ELO.

15. SUBJECT TERMS
epitaxial growth, III-V semiconductors, semiconductor epitaxial layers, semiconductor growth, photonic integrated circuits, epitaxial layer overgrowth, heteroepitaxy.

16. SECURITY CLASSIFICATION OF:			17. LIMITATION OF ABSTRACT:	18. NUMBER OF PAGES	19a. NAME OF RESPONSIBLE PERSON (Monitor)
a. REPORT	b. ABSTRACT	c. THIS PAGE			Vassilios Kovanis
Unclassified	Unclassified	Unclassified	SAR	26	19b. TELEPHONE NUMBER *(Include Area Code)* N/A

Epitaxial Hybrid Silicon Laser Technology

Final Performance Report, FA8650-10-1-7031

Abstract

We have investigated a wide range of conditions for MOCVD epitaxial layer overgrowth, and studied the impact on coalescence on the ELO patterns and orientations. We have found conditions that allow us to grow such that the coalesced regions are defect free. This is a first for MOCVD and it is the first for growth across a significantly wide field.

The fundamental nucleation and growth of As and Sb based III-V semiconductors on SiO_2 masked Si(100) and InP(100) surfaces were investigated via molecular beam epitaxy (MBE) to determine the best growth windows for nucleation and lateral overgrowth. Antimonides provide better lateral overgrowth than arsenides indicating transitions from layer-by-layer to step flow growth regimes in MBE may be critical for ELO.

1. MOCVD effort

1.1 Introduction

The main advantage to doing epitaxial lateral overgrowth (ELO) using MOCVD or CBE methods is the ability to grow laser structures directly after establishing the high quality ELO film. However, in our literature searches we have not found any papers showing the successful MOCVD or CBE growth of continuous InP or GaAs films with a high fraction of ELO material vs. material grown directly over the seed material. Namely, there has been no reported success of forming coalesced regions of significant width on the micron or tens of micron scale. In general, such papers show the growth of ELO stripes that at best come close to touching their neighboring stripes [1]. Beyond the ability to coalesce the stripes at all when there is significant lateral growth, there has also been the question of defect formation at this coalesced front since groups finding success in filtering defects within growth window find significant defect formation at the coalescence point [2].

These factors come into play regardless of the size of patterns through which growth from the seed layer occurs or the seed layer below the patterning. Because of this, these factors have been the focus of our work, which we performed on InP substrates due to the large number of growths needed. Similarly we have found that the use of our 0.8μm openings presented a situation quite different from earlier ELO investigators' work using openings of 5μm and larger. Namely, the stripes were narrow enough that it was not necessarily possible to distinguish between edges and centers of stripes when the sidewalls of growing material were so close as to constitute the whole of the stripe. This is a situation that will only become more important with the shrinking of the window width. Shown in Fig. 1 is the result of applying typical growth conditions used by prior MOCVD growers using wide windows rather than the narrow windows we use. To summarize what has happened, the film has emerged from the window with a geometry such that the lateral growth-limiting {111} planes quickly become the majority surface area or even completely eliminate the higher growth rate planes. Further deposition follows a very disordered pattern dominated by stochastic nucleation mechanisms rather than the orderly step-flow conditions normally present in planar MOCVD.

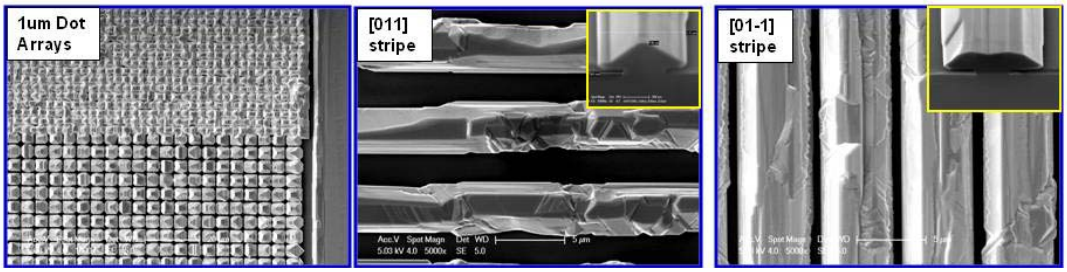

Fig. 1 Examples of growth results when growing through very small windows using conditions from earlier work using MOCVD. Small windows quickly lead to growth profiles where most of the available surface is a low growth plane and disordered growth results.

As described below, we have achieved this goal of creating a continuous film with an ELO-to-Seed area ratio greater than 5. We have also shown that proper conditions can lead to a film where there are no observed coalescence defects. On this film we have grown 5 quantum well structures and found that the strength of the PL signal is comparable between coalesced regions and open field regions. These results were only semiquantitative owing to variations in surface heights across the different patterns, but they imply that there is little or no introduction of defects at the coalescence fronts. We also characterized different coalescence results via cross-sectional TEM to find that the introduction of defects at the coalescence front can be controlled.

1.2 Identification of key growth behaviors

In our early work on this contract, we identified patterns in growth laterally from the stripe as related to basic growth parameters. These conclusions were drawn from relatively thin growths that showed the stripe development right after the grown layer. The thickness of these films was 0.3μm of Open Field Thickness (OFT)—the thickness that would be deposited in areas without any masking InP. Also included in these early observations were many anomalies that seemed to oppose the initial observations, especially with regard to the tendency of films to coalesce along particular directions and the quality of sidewalls. Because of these observations we made multiple growths of thicker layers and larger variations in growth parameters. In doing so we identified the best criteria for characterizing the growth habit. Upon doing so we were able to identify fully consistent behaviors which depend on the strongest factors of stripe direction and V/III ratios.

The ways growth behaviors vary are best summarized by plan view images of thicker growths on our so-called wagon wheel growth patterns. In these patterns, 0.8μm windows in the SiO_2 mask were opened as rays of constant width with angular separations of 5.625° (1/64 of 360°). Besides giving an overview of the dependencies on stripe direction, these thicker growths also show the ability of stripes with different directions to coalesce.

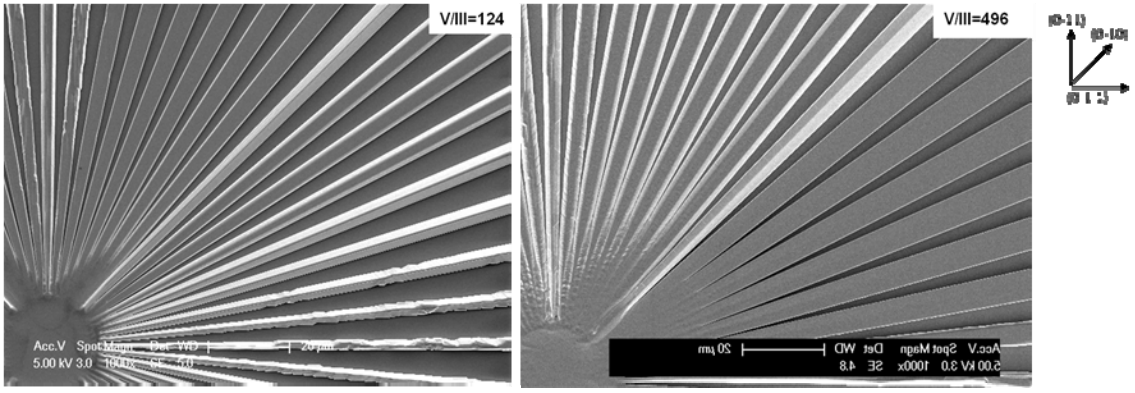

Fig. 2 "Wagon wheel" growth patterns showing apparent "flipping" of the stripe shapes of the stripes closer and farther from vertical than the 45° or [0-10] direction. V/III ratios are as indicated upper right in each picture. The picture for V/III=496 has been flipped for ease of comparison but was taken from a crystallographically equivalent location on the wheel.

Fig. 2 shows how the stripe orientation and the V/III ratio combine to show a variety of behaviors. The most obvious apparent differences in these SEM photos is that the flat-topped stripes for the lower V/III ratio are closer to the (0-11) direction than the highly faceted, pyramidal (0 10) ("45°") stripe while the opposite seems true when the V/III ratios is very high (496). Similarly, the stripes "north" of the 45° stripe are showing coalescence when V/III=124 while the stripes south of the 45° show smooth coalescence. Though not pictured here, the coalescence of the stripes north of the 45° is severely hampered at the more moderate V/III ratio of 248. Another difference is that the sidewalls do not show up on the very flat topped stripes while there seems to be a facet developing with some vertical component on the stripes with the bright edges.

While one would expect there to be changes with respect to V/III ratio, the complete reversal of crystal growth habit seems unlikely. To address this we did a wide survey of samples looking at many different characteristics for characterizing the samples and found what is shown in Figure 3. The classification system presented finally yielded systematic results for any thickness and condition, with small variations from lesser effects such as growth rate.

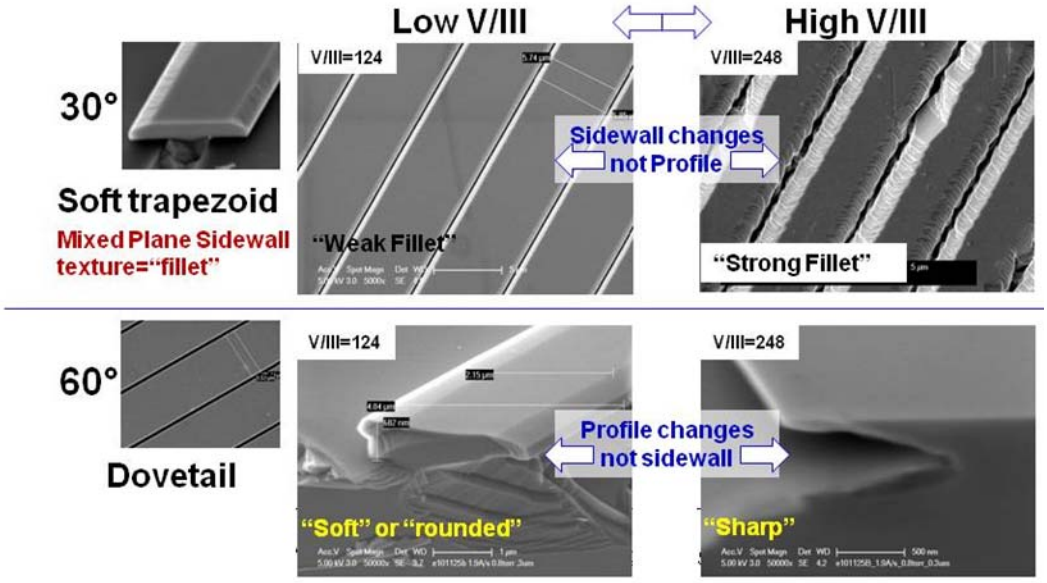

Fig. 3 Shown above are the four quadrants of general shapes found when looking at growths on stripes near the [0-10] direction with the 30° direction indicating 30° off of [0-1-1]. The use of plan view or cross-section coincides with what view is needed to best evaluate the changes taking place on a certain set of directions and V/III ratios

Namely the stripes closer to the [0-1-1] ("south of 45°") direction consistently have an appreciable amount of undercut in cross-section and very smooth/straight sidewalls when viewed from above. In the figure below, these are the 60° stripes as the angle is measured from [0-11]. In the case of high V/III ratios, when coalescence is best observed, the 60° stripes' undercut is very well defined and presents as a very sharp dovetail cross-sectional profile. Varying the V/III ratio for these stripes changes the cross-sectional profile but has little effect on the sidewalls when viewed from above. Thus these stripes are best analyzed with cross-sections to qualify the stripes. The opposite is true for the stripes having a direction closer to [0-11]. The profile of these 30° stripes shows little change while the sidewalls are strongly affected by the V/III ratio such that plan view views are sufficient for qualifying these stripes. We refer to this texture as a fillet structure, which is best seen in the upper right picture. At the equivalent magnification for the lower V/III ratio it is barely visible. In the end, both of these attributes affect the lateral growth speed and the ability of a set of stripes to coalesce. The fillets themselves appear to consist of {010} planes which are both high growth planes and yet strongly affected by neighboring {111} planes, which partially constitute the steps between "scales". In summary, we have found that it best to characterize stripes according to their cross sectional profile, as either "soft trapezoidal" or "dovetail", and according to their sidewall appearance from above as either "filleted" or "smooth/straight". In addition, we find that the stripes closer to the [0-11] direction are more strongly affected with respect to the sidewall while the stripes closer to the [0-1-1] direction are more strongly affected in terms of cross sectional profile.

1.3 Coalescence Studies and Conclusions

Using the observed patterns, we were able to design a focused study to characterize the effects of the changes in growth habit shown above on lateral growth rate and coalescence. We varied growth

rates from 0.5-8Å/s, with 4Å/s being our normal rate for planar growth of InP. Group V factors were a variation of V/III from 82 to 496 and variations of absolute TBP pressures from 0.87 to 4.1torr. Absolute chamber pressure was also tested at atmospheric pressure and 76torr besides the normal operating pressure of 350torr.

Fig. 4 shows the relationship between lateral growth rate and V/III ratio. These data were taken at an Open Field Thickness (OFT) of 0.9μm so that effects of decreasing loading from the shrinking SiO_2 mask are not a strong factor. From the graph it is clear that the rate increases as V/III increases until a very high ratio is reached. It is possible that there is an optimal ratio near 400 but it is also important to note that the point at V/III=500 could be affected by that fact that even though the V/III ratio was high, the absolute TBP pressure was lower than the V/III=406 data point. In any case, these results were useful in achieving our coalesced films with a minimum of OFT.

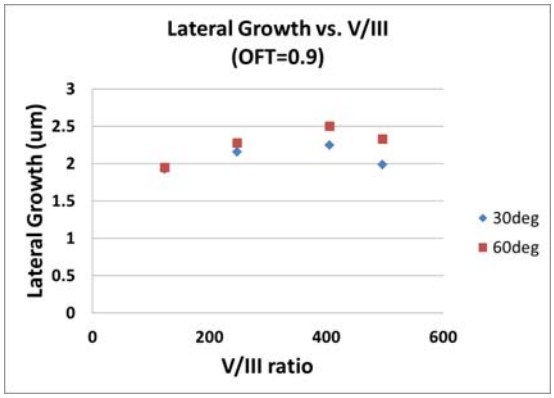

Fig. 4 Variation of Lateral growth as a function of V/III ratio. Besides the trend of increasing lateral growth it can be seen also that the difference between the two directions increases with the 30° direction becoming relatively slower.

From Fig. 4 it is also important to note that the difference between the 30° and 60° stripes increases with the increasing V/III ratio. This correlates with the increasing "fillet" texture on the 30° stripes' sidewalls and shows up later with drastic consequences when the stripes near coalescence. At the same time, the 60° stripes are becoming more sharply defined as a dovetail shape.

While other groups have studied to a limited extent the effects of conditions on lateral rate and the cross-sectional profile of ELO growth, coalescence studies for MOCVD growth are conspicuously absent. The best study on lateral growth habit and profile development achieves time resolution of long growths by periodically doping the growth for SEM contrast [3]. Doping distributions however can be fickle when doing non planar growth and growths closer to coalescence will likely exacerbate this problem. Instead, we have selected to grow multiple series of growths stopping each growth at a different time.

The results of these growths at two moderate to high V/III ratios (124 and 248) are shown in Fig. 5. These results are representative of our other series and are also the V/III ratios closest to our normal growths. Immediately it is clear that the higher V/III ratio lateral growth is higher to begin with. Furthermore, as observed in Figure 4, the difference in growth for the 30° and 60° is very clear at the higher V/III ratio. The general shape of these curves is what one would expect from a perspective of loading. Basically as the stripe grows and nears coalescence, the amount of excess

TMI / In that can diffuse from the mask decreases since the space and area of SiO_2 between the stripes decreases.

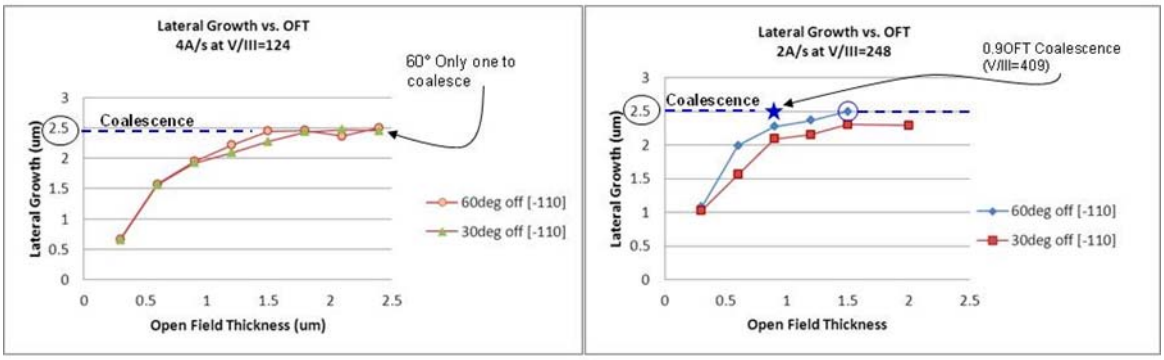

Fig. 5 Examples of thickness/coalescence series growth for two V/III ratios. SiO_2 field width is 5µm requiring lateral growth of 2.5µm Single point from a very high V/III ratio growth (409) is represented with a star indicating the fastest coalescence achieved in this study.

This loading effect explains the general "roll over" trend, however it does not explain the way some curves appear to reach a saturation point rather than coalescing. This saturation is most obvious on the 30° stripes grown at a higher V/III ratio of 248. It is, however, also present on the V/III=124 graph, though it is hard to recognize since the data lie very close to the exact 2.5µm point of coalescence. It is also clear on the 60° data set. However, the key point is that the stripes along the 30° direction do not coalesce and have not been shown to coalesce across the 5µm fields in any of our studies for parallel lines.

This reluctance to coalesce correlates directly with the appearance of fillet texture as shown in Fig. 3. Just as the fillet structure is most pronounced at higher V/III ratios, the reluctance to coalesce is much more clear as well. Thus, we show that the development of the fillet structure interferes with the coalescence of parallel lines. It is also worth noting that a closer inspection of the wheel structures show stronger fillet structure in areas close to coalescence than further out on the spokes. In these situations, the same growth time has occurred but the stripes are farther apart. Thus the development of the fillet structure appears to be more strongly correlated with proximity of neighboring stripes than with time and thickness of growth. Likely, it is related to the local reduction of excess In and P in a region where multiple growth planes are clearly in competition. This is supported also by observations reported early in this program of increased faceting at very low TBP and TMI pressures.

In the V/III=124 series the 60° stripes are reluctant to coalesce and show a saturation effect. However, these stripes do eventually coalesce albeit with a growth of OFT nearly equal to the lateral growth. A set of these stripes at this saturation point are shown in Fig. 6. Unlike the 60° stripes at higher V/III ratios or these stripes earlier in their approach to coalescence, the sidewalls are no longer smooth. Thus the sidewall structure is critical to coalescence, and the low V/III ratios will not favor coalescence along dovetail stripes.

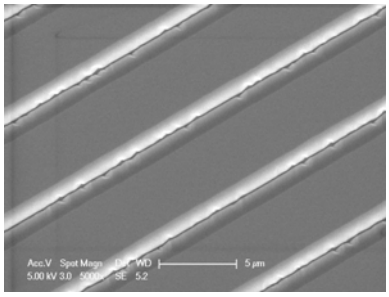

Fig. 6 60° off of [0-11] stripe near coalescence at V/III=124 showing development of sidewall features.

1.4 Optimized Coalescence and Characterization

From the studies above we found that the stripes with the fillet structure and trapezoidal cross section will not coalesce across a large field, though coalescence observed across narrow fields such as 1μm was observed (OFT was greater than 2 times the needed lateral growth). Lower V/III ratios could mitigate this by decreasing the strength of the fillet structure on these stripes. On the other hand, the low V/III ratios lead to weakening of the dovetail stripes cross section as well as the development of sidewall features also detrimental to coalescence. From this we found that, while most investigators focus on the cross section of the ELO stripes, the sidewall smoothness/straightness is critical to coalescence.

With this information we sought to grow the thinnest possible ELO film that would result in a fully coalesced film. Our best result is represented by the star on the V/III=248 graph but is actually a growth done at a V/III ratio of 409. This best effort required only 0.9μm of OFT growth, which corresponds to a lateral to vertical (nominal) growth rate ratio of 2.8. Fig. 7 shows a cross sectional SEM. Unfortunately, cleaving often leads to chipping of the SiO_2 field but the chipped away areas correspond to the ELO portion of the film. The dovetail shape is still present indicating that coalescence occurred only at the top of the mesas. The picture was taken near the edge of the pattern field where excess loading is decreased. The excess delivery of reactants is less on the right side of the picture owing to there being an open InP field nearby rather than the simply more masking pattern as is true for the left side of the picture. The result is a picture showing the moments just prior to coalescence and the rapid planarization of the film.

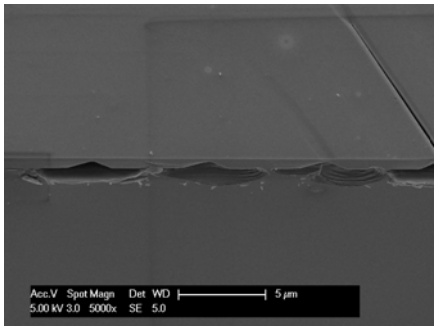

Fig. 7 Cross section of coalesced film across 5μm wide SiO_2 fields along 60° off of [0-11]. Picture is taken near edge of pattern field to show coalescence stages.

It was on a film grown under these conditions that we grew a set of quantum wells at 1.55μm. A quick measurement verified that the strength of the PL in high quality (sharp dovetail) coalesced

regions was the same wavelength within a few nm and comparable in intensity to the wells on the planar InP region. These measurements were only semiquantitative owing to difficulty of using the set up to compare measurements on regions of different heights. We are in the process of making these measurements more quantitative.

To further characterize the quality of coalesced regions we performed TEM on coalesced regions of the wheel structures. The coalescence phenomena of the stripes on the wheels is different from that of parallel stripes since the wheel spokes are not parallel but rather have a small opening angle of 5.625°. However, the zipper-like coalescence one expects from such an arrangement has been shown to yield coalescence between stripes on both sides of the 45° stripe (ref Fig. 2). Thus we can directly compare coalescence of smooth sidewall (dovetail) stripes to coalescence of fillet structured stripes.

Fig. 8 shows multiple cross sectional TEM views of coalesced regions near the 45° [0-10] stripe and center of a wheel structure. The four pictures correspond to the four combinations of Trapezoid vs. Dovetail profiles and high vs. low V/III ratios. Here "trapezoid" is shorthand for the stripes showing fillet sidewall structure with directions near the 45° or [0-10] direction but closer to [0-11] such as the 30° stripes above. Likewise "dovetail" denotes the stripes such as the 60° stripes closer to the [0-1-1] direction.

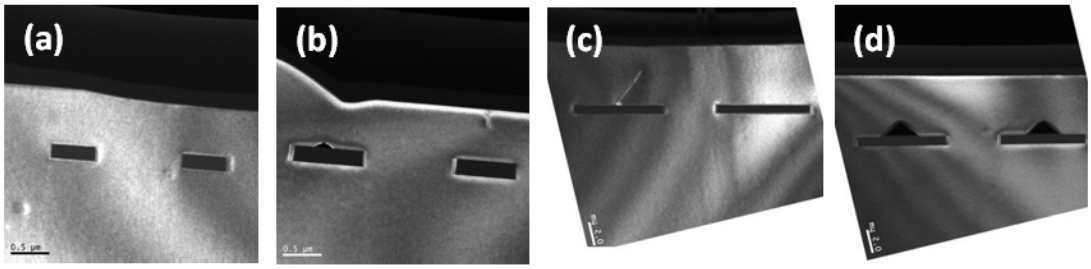

Fig. 8 Cross sectional TEM views of coalesced region near the 45° or [0-11] direction. The black rectangles are the SiO_2 mask regions so InP above is coalesced ELO material. Views are as follows: a) stripes closer to [0-1-1] or trapezoid/fillet with V/III=124; b) stripes closer to [0-11] or dovetail with V/III=124; c) trapezoid/fillet stripes, V/III=248; d) dovetail stripes with V/III=248.

The first two pictures (Fig. 8(a) and (b)) correspond to coalescence at the lower V/III ratio of 124. Under these conditions the stripes have a weaker fillet structure and can coalesce in these situations of the stripes not being parallel. Furthermore, no defects are observed for these stripes. On the other hand, as Fig. 3 and Fig. 6 show, the V/III=124 situation leads to poorer sidewall smoothness and shaping for the dovetail stripes. Fig. 8(b) shows defects for both the situation where the dovetails have met and coalesced primarily at the top (very faint) and the situation where roundedness apparently allowed for coalescence at the bottom of the mesa structure as well. The excess thickness on the left hand side is a result of the dovetails being much more sensitive to directional variation so that the stripe to the left has a very different profile (see the first wheel in Fig. 2).

Fig. 8(c) and (d) show the situation of high V/III ratio growth. In this case the fillet structure is greatly enhanced and leads to clear defects as shown in Fig. 8(a). Occasionally defects are not found due to the low sampling volume of a cross sectional TEM and the way that fillet structured sidewalls meet first at points spaced out according to the period of the "scales". However, consulting multiple coalescence regions makes the pattern consistent. As we would expect we did

not find defects in the regions where dovetails met under high V/III conditions since the sharp dovetails shape leads to initial contact only at the very thin upper corners of the mesa while the smoothness along the length of the sidewall yields less opportunity for voids as found in rough sidewall coalescence.

What we have shown here is that coalescence is indeed a critical stage to consider since defects are formed, even when the films are grown on InP wafers. The conditions we have specified, however, allow us to grow such that the coalesced regions are defect free. Not only is coalescing with MOCVD across a significantly wide field is a first, we can also say that this can be controlled such that defects can be avoided.

1.5 InP on Si growth

We currently have three types of planar InP-on-Si samples. The first of these are those we have developed in house. Since we have found sources of samples with InP on Si we have focused less on growing our own InP coated Si wafer and more on the ELO studies above. Nonetheless, we have done growths enough to have identified growth windows that seem to be unique to the situation of using TBP instead of PH_3 as used by all other previous investigators.

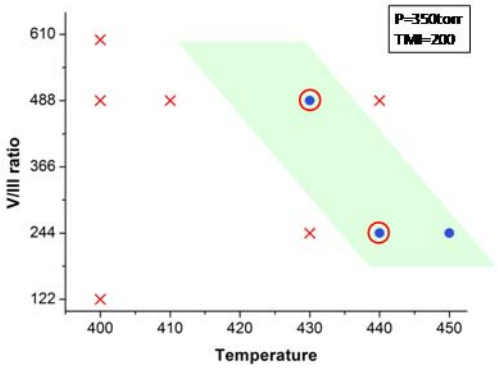

Fig. 9 Summary of InP growths at low temperatures. "X" symbols denote poor surface morphology while dots indicate good morphology and circles are repeated growths.

Fig. 9 summarizes our initial growth results of low temperature InP growths necessary for growing the first buffer layer on Si. The "x" marks denote poor surface morphology while the dots show mirror-like morphologies and circles denote repeated growths. As expected, very high V/III ratios are needed at low temperatures. From the trend, it seems that the V/III ratios will be very large at our target temperature around 400°C. We have modified our reactor to allow for very high TBP flows but will still need to modify our growth procedures and rates if we are to follow the indicated trend.

One observation worth noting is the result where the higher V/III ratio at 440°C actually worsens the morphology. This has not appeared anywhere in the literature and could possibly be related to the use of TBP instead of PH_3. In any case, it goes against common knowledge regarding the effects of group V pressures. It is also surprising to find an apparent need for such high V/III ratios

given that earlier workers' use of PH_3 meant dealing with very low cracking efficiencies, especially compared to TBP with its lower dissociation temperature.
One of the reasons for our recent investigations into growing our own InP seeded Si wafers has been issues with poor morphologies on wafers received from outside sources. Our first supplier (Spire Semiconductor) used a simple two step process of a low temperature GaAs nucleation layer followed by 1.5μm higher temperature growth of InP. The result was a specular surface but with a haze that shows up in Nomarski as shown in Fig. 10. The right hand picture shows the result of growing on such a rough substrate. What we have found is that such starting roughness leads to growth from the window that replicates the roughness in such a way that the stripes show the development of structures similar to that found in early growth along the <011> directions. Namely low surface energy facets nucleate early and lead to only very slow, if any, ELO growth. Interestingly, the resulting stripe morphologies do show some directional dependence and are not simply replications of the underlying seed layer's morphology.

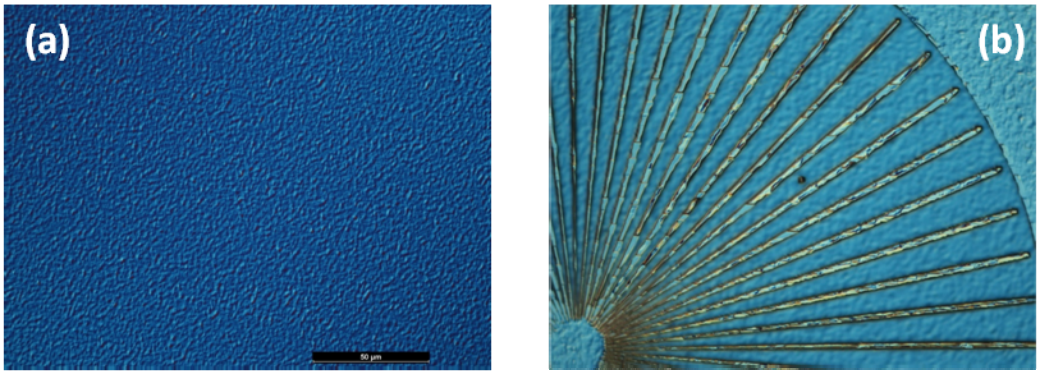

Fig. 10 (a) shows the surface morphology of InP grown on Si using a simple two-step method. (b) shows attempted ELO growth with the formation of disorded arrays of low surface energy (low growth rate) planes that hinder lateral growth.

On a subsequent DARPA MTO contract that is continuing, we purchased a new set of samples that were grown by another outside source (IQE). These wafers utilized a more complex seed structure known as an M-buffer sequence. These layers consist of a GaAs buffer layer followed by an InAlAs layer with graded composition from lattice-match to GaAs to just beyond the lattice constant of InP. This resulted in much better quality material as shown in Fig. 11. Growth on these substrates will be conducted and reported on that contract.

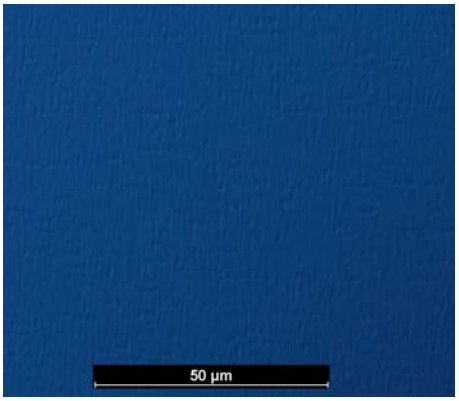

Fig. 11 Higher quality InP-on-Si wafer grown using an M-buffer method.

1.6 MOCVD ELO Summary

We have investigated a wide range of conditions for epitaxial layer overgrowth, and studied the impact on coalescence on the ELO patterns and orientations. We have found conditions that allow us to grow such that the coalesced regions are defect free. Not only is coalescing with MOCVD across a significantly wide field a first, we can also say that this can be controlled such that defects can be avoided. These results have been submitted to the Journal of Electronic Materials[4] and were presented at the Electronic Materials Conference[5,6].

1.7 References

[1] Zhou J. et. al, Surface characterization of epitaxial lateral overgrowth of InP onInP/GaAs substrate by MOCVD, Microelectronics Journal 38 (2007) 255–258

[2] Langudo T.A. et. al, High quality Ge on Si by epitaxial necking, 76 no.25 (2000) 3700-3702

[3] Sun Y.T. et. al, Temporally resolved selective area growth of InP in the openings off-oriented from [110] direction, Journal of Crystal Growth 225 (2001) 9-15

[4] Julian, N., Mages, P.A., Zhang, C., Zhang, J., Kraemer, S., Stemmer, S., Denbaars, S., Coldren, L.A., Petroff, P., Bowers, J.E., "Coalescence of epitaxial lateral overgrown InP by MOCVD with v/iii ratio variation", submitted to Journal of Electronic Materials, 2011

[5] Julian, N., Mages, P.A., Kraemer, S., Zhang, J., Stemmer, S., DenBaars, S. P., Coldren, L.A., Petroff, P., Bowers, J.E., "Coalescence phenomena in narrow-angle stripe epitaxial lateral overgrown InP by MOCVD", Electronic Materials Conference, 2011

[6] Mages, P.A., Julian, N., Zhang, C., Coldren, L., DenBaars, S., Bowers, J.E., "Growth habit control of epitaxial lateral overgrown InP on Si substrates by MOCVD", Electronic Materials Conference, 2011

2. CBE and MBE effort

2.1 Introduction

During this program, the fundamental nucleation and growth of As and Sb based III-V semiconductors on SiO_2 masked Si(100) and InP(100) surfaces were investigated via molecular beam epitaxy (MBE) to determine the best growth windows for nucleation and lateral overgrowth. Solid group-III and group-V atomic and molecular sources were used to provide an understanding of the temperature dependent surface mobility and bonding preferences of the elements on the various surfaces. The use of solid sources reduces the degrees of freedom that gas sources in chemical beam epitaxy (CBE) provide, but identifies where the most promising growth windows may be found. CBE growth is powerful in combining surface selectivity with atomic level growth control, but growth windows can be very sensitive to temperature and fluxes and consequently, easily missed. The growth windows identified from MBE and MOCVD will enable a growth window from CBE to be found. Under this program the following was accomplished this past year:

- Surface preparation of atomically clean Si surfaces for MBE and CBE growth by ex-situ etching of the surface SiO_2 by dilute HF and in-situ annealing.
- Si surfaces sufficiently clean to allow epitaxial overgrowth growth of GaAs by MBE
- GaAs films on SiO_2 masked Si(100) surfaces showed preferential nucleation on the cleaned Si(100) surfaces with respect to the SiO_2 hard mask for growth between 450ºC and 650ºC.
- No significant coverage of SiO_2 surfaces at 450ºC growth conditions for InAs, GaAs, and InGaAs when nucleated on InP(100)
- Antimonides provide better lateral overgrowth than arsenides indicating transitions from layer-by-layer to step flow growth regimes in MBE may be critical for ELO.
- A CBE system was brought up to near operational condition in preparation for ELO growth studies.

2.2 Preparation of Patterned Silicon Substrates

The silicon wafers, following processing must have the open surface areas prepared prior to epitaxial growth. The patterning and subsequent transfer of the wafers results in both the formation of a surface oxide and in hydrocarbon adsorption. Although the proposed overgrowth does not require a perfectly clean surface and interface, there must be sufficient areas of epi-ready Si exposed to properly nucleate InP growth. A series of UHV cleaning and annealing processes were evaluated using in-situ surface characterization techniques.

Traditional Shiraki cleaning methods for Si wafers are not directly applicable for the processed wafers as the cleaning process would also attack and degrade the silicon dioxide hard mask structures as well as the exposed Si. As a result we explored the use of in-situ hydrogen cleaning of the wafers to remove carbon traces and a substrate annealing stage to examine the removal rate of the native Si oxide left on the exposed areas. An atomic hydrogen source was attached to the MBE deposition and characterization system. The source flows H_2 through a leak valve into a 1950ºC cracking tube and the atomic hydrogen then impinges on the wafer. The wafer itself is held in a standard growth manipulator that can reach 725ºC with current power sources and capable of reaching slightly higher than 800ºC with a higher power source.

As an initial step to qualify the various stages of the process we began by simply looking at the surface of unprocessed Si wafers. A Surface Science Labs x-ray photoemission spectroscopy (XPS) system also attached to the UHV system is being used to examine the resulting surface effects from hydrogen cleaning, annealing, and following subsequent growth. The wafers are first brought into

the system, outgassed at 200ºC to remove water vapor and light volatiles. They are then to be annealed around 500ºC-600ºC under the atomic hydrogen flux, which will remove any carbon contaminants left on the surface. If not removed, additional heating will result in reactions of the carbon with the substrate to produce SiC. A part of the characterization being done now on the unprocessed wafers and eventually on the processed wafers is to characterize with XPS, how much carbon is typically present. Following the hydrogen clean, an anneal was performed to remove the native surface oxide. This process worked well in removing the residual carbon, but the high temperature anneals required (>800ºC) was not well suited for indium or gallium bonding used to mount samples to our molybdenum substrate holders. As a result, ex-situ preparation techniques were also examined.

Fig. 12 shows x-ray photoemission spectroscopy (XPS) taken in-situ of the Si(100) surface from an unprocessed commercial silicon wafer after various treatments. The top spectrum shows the oxide present on an untreated wafer following an anneal in vacuum at 250°C to remove any residual water vapor from the surface. The second spectrum shows that following an 800°C in-situ anneal, there is almost no reduction in the surface oxidation. The last spectrum shows a surface prepared ex-situ by using a dilute HF:H_2O etch of approximately 1:25 for approximately 45 seconds, rinsing in DI water, and drying with nitrogen. The etch rate was determined to be ~8 nm/min at this concentration by measuring the thickness of the native oxide after successive 10 second etching intervals via spectroscopic ellipsometry. The wafer was then loaded into vacuum and annealed for 2 hours at 250°C prior to XPS characterization. The spectrum shows significant reductions in oxygen indicating the etching step and subsequent hydrogen termination is effective in producing a nearly oxide free surface. Low energy electron diffraction of the same surface reveals a strong 1×1 pattern indicative of a highly ordered crystalline surface suitable for epitaxial growth.

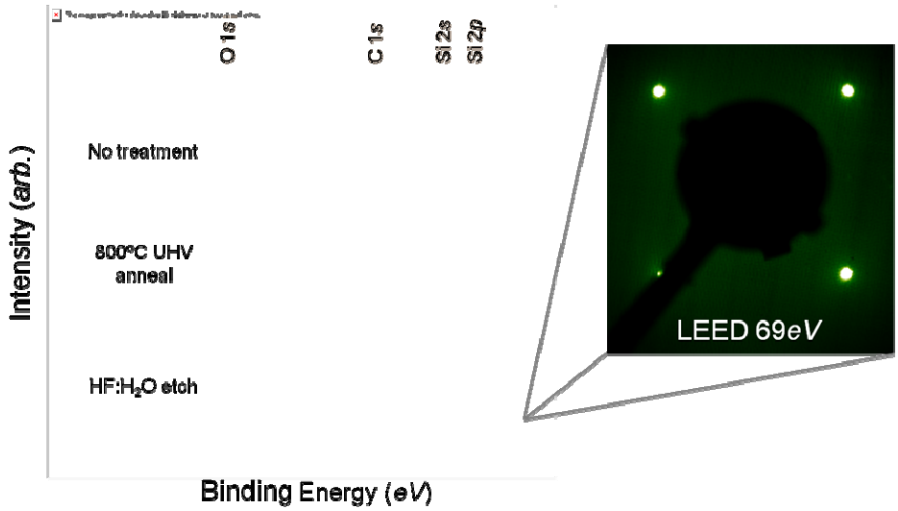

Fig. 12 XPS spectra following various surface treatments of silicon wafers. The use of an ex-situ dilute HF etch produced a nearly oxide free surface with good crystalline order as shown by the in-situ LEED pattern.

2.3 MBE Growth on Silicon(100) Substrates

Fig. 13(a) shows Reflection High-Energy Electron Diffraction (RHEED) pattern from a Si(100) surface along an <011> prepared via a dilute HF:H_2O etch described above. The pattern was acquired in an MBE system at 450ºC and shows a strong 1× pattern consistent with the LEED

pattern in Fig. 12. A weak 2× pattern also begins to appear at these temperatures consistent with a (1×2)/(2×1) surface reconstruction of Si resulting from the desorption of hydrogen, which is expected to occur by 425ºC [1].

MBE growth of GaAs was initiated on the Si(100) surface at 450 ºC. An As flux produced no visible change on the surface at this temperature, but subsequent exposure to a Ga flux resulted in GaAs growth on the surface. Fig. 13(b) shows the RHEED pattern taken along the <011> direction following 3 nm of GaAs coverage. The spotty pattern is indicative of 3D growth. Fig. 13(c) and (d) show the respective RHEED patterns following 400 nm growth at 450ºC and following 700 nm of growth at 530ºC. The last pattern shows a more streaked pattern suggesting the 3D island growth has begun to coalescence. The (2×4)/(4×2) pattern visible in the RHEED pattern is consistent with that of an arsenic rich reconstructed (2×4)/*c*(2×8) GaAs(100) surface. These results provide a point of reference for growth on the SiO_2 patterned surfaces that we have fabricated.

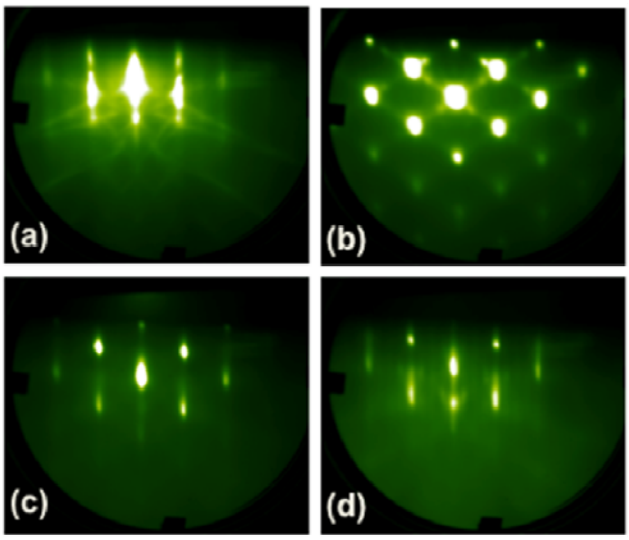

Fig. 13 RHEED patterns obtained during the growth of GaAs on a Si(100) wafer (a) before growth along the Si<011>, (b) after 3nm of GaAs growth at 450ºC, (c) after 400nm of GaAs growth at 450ºC, and after 700nm of growth at 530ºC.

2.4 MBE Growth on SiO_2 Pattered Si(100) Surfaces

The growth of GaAs on patterned Si(100) substrates was investigated to determine whether the surface selectivity of elemental Ga and As sources was sufficient to enable preferential growth of GaAs on Si with respect to masked areas of SiO_2. The growth of III-V compound semiconductors on SiO_2 patterned Si surfaces by solid source MBE requires finding a growth window where the mobility of the elements on the SiO_2 are sufficient to prevent growth on the hard mask, while still promoting growth on the clean Si surfaces. A second growth window is subsequently required to encourage overgrowth of the masked areas once the growth has extended above the height of the mask. We have begun to look at the growth of GaAs on these masked surfaces. Fig. 14 shows optical micrographs of masked Si surfaces following 50nm of GaAs growth by MBE at (a) 650ºC, (b) 625ºC, and (c) 450ºC and Fig. 14(d) following 500nm of GaAs growth at 550ºC. For all four growths, the growth rate was held constant at 3 nm/min. The high temperature growth showed no change in the RHEED images during growth, and the optical images showed no evidence of growth at 650ºC indicating that the desorption rate of the elements at 650ºC was higher than the deposition

rate. However, by lowering the substrate temperature to 625ºC, growth was found to occur on the Si surfaces, but not on the SiO_2 surfaces. Images show large grain growth, and RHEED suggests the GaAs is polycrystalline. Additional work is still needed to improve the crystallinity of the Si surfaces on the processed wafers before growth. The selectivity of the growth indicates the Si surface is sufficiently different from the SiO_2 areas to promote growth, but not sufficient to nucleate preferentially oriented GaAs. Growth as low as 450ºC still showed no growth on the SiO_2 indicating the GaAs has a fairly large growth window for nucleation by solid source MBE. Optical images show uniform coverage of the Si areas, and RHEED suggests growth is still polycrystalline. Extended growth times resulting in half a micron of coverage at 530ºC produced a surface completely covered by the GaAs. Fig. 14(d) shows an area of the specimen masked during growth showing complete coverage where exposed to the GaAs and no growth where masked. These growths show that there is definitely a window for nucleation and for lateral coalescence of GaAs films grown on masked Si(100) surfaces.

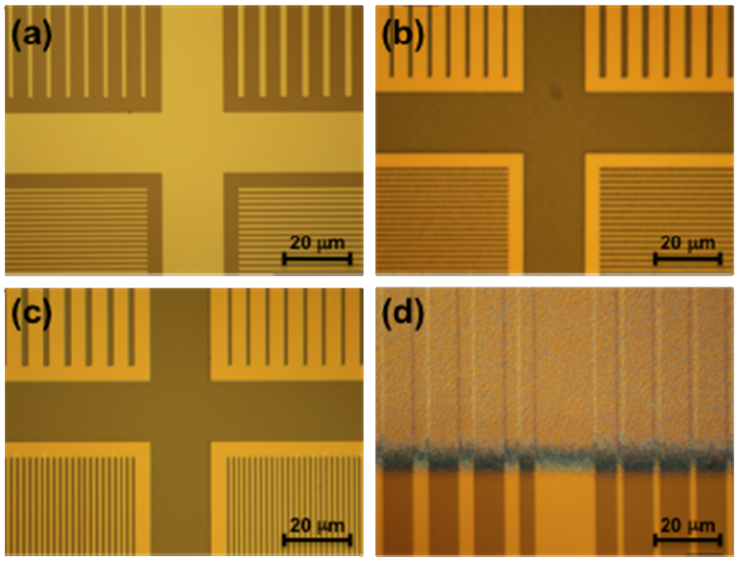

Fig. 14 Optical images of SiO_2 masked Si(100) surfaces following GaAs growth of (a) 50nm at 650ºC, (b) 50nm at 625ºC, (c) 50nm at 450ºC, and (d) 500nm at 550ºC.

2.5 MBE Overgrowth of Patterned InP(100) Surfaces

Since MBE was able to provide some surface selectivity for growth on SiO_2 masked Si, we focused on determining whether the growth of lattice matched (In,Ga)As on patterned InP(100) surfaces provided any of the same surface selectivity for elemental In, Ga and As needed to enable preferential growth with respect to masked areas of SiO_2 at temperatures where InP remains stable. The first step to overgrowth was to be able to prepare the InP surfaces for growth following processing. The native oxide for InP left after the deposition of the SiO_2 mask is relatively thin, which is both an advantage and disadvantage. The mask contains an open area of a few square mm to allow RHEED to be used during MBE growth. Fig. 15(a) shows the RHEED pattern attained along the [011] in-plane direction from the patterned InP(100) surface. The RHEED shows a fairly streaky pattern indicating the surface is well ordered. The thin oxide still on the surface is removed in the MBE by heating the sample under an arsenic flux (typically As_4). The arsenic is used to help stabilize the surface during the thermal anneal. The difficulty of the thin oxide, is that it is not always clear when it has been thermally desorbed removed. To assure proper oxide removal, the

samples were heated slowly (5-10ºC/min) to approximately 530ºC at which point the surface changes from a 2x ordering to a more indium rich 4x as seen in Fig. 15(b). The sample is then promptly cooled to 480ºC and the surface is found to quickly reorder back into a more As rich 2x as seen in Fig. 15(c). The surface is then clean and ready for epitaxial growth.

Initial growths were performed on the patterned InP(100) surface for InAs, GaAs, and lattice matched InGaAs. InP has a lattice parameter of 5.8686Å, while InAs is 6.0584Å (3.2% larger), GaAs is 5.6533Å (3.6% smaller), and In0.53Ga0.47As is lattice matched. Fig. 16 shows the RHEED along the two principle <011> directions and optical microscope images following 100nm of InAs, GaAs, and $In_{0.53}Ga_{0.47}As$ growth at 480ºC on InP(100) surfaces patterned with 60nm high SiO_2 features. The RHEED in all three cases shows epitaxial oriented films confirming that surface oxide of InP was removed, and that the material is growing coherently on the underlying substrate. Following growth, the surfaces were annealed for 5 minutes at 480ºC and then cooled to 300ºC while exposed to a continuous arsenic flux. Once the surface temperature reached 300ºC, the arsenic was valved off and shuttered and the samples were annealed for 20 minutes while the background chamber pressure fell into the 1×10^{-10} mbar range.

The RHEED images in Fig. 16 correspond to the sample surfaces just prior to being removed from the MBE chamber. Surface reconstructions for all three cases show excellent coherence with the underlying InP. The exposure to arsenic at 300ºC produces different surface reconstructions for the three materials. For example, InAs terminates in a (2×4) order surface, GaAs in a *c*(4×4) surface, and the InGaAs terminates in a (4×3). The RHEED images are sharp and well defined indicating that the growth of all three materials was quite good. The RHEED images also do not show any significant indication of "ring" formation in the patterns, which would be indicative of polycrystalline growth on the SiO_2.

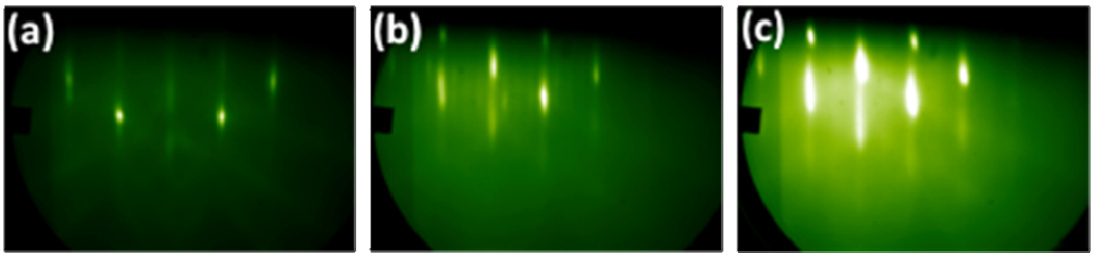

Fig. 15 RHEED images of the patterned InP(100) surface along the [011] direction (a) as loaded into vacuum and heater to 300ºC, (b) after heating to 530ºC under As_4, and (c) after cooling to 480ºC under As_4.

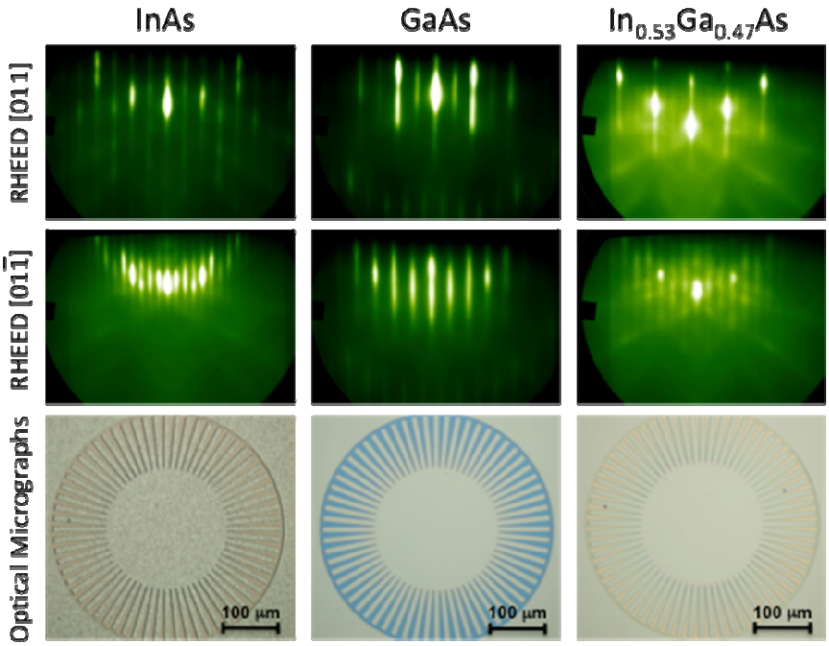

Fig. 16 Shows RHEED along the two principle <011> directions and optical microscope images following 100nm of InAs, GaAs, and In0.53Ga0.47As growth at 480ºC on InP(100) surfaces patterned with 60nm high SiO_2 features.

Despite the fact that the RHEED for the InAs growth suggests that the surface is flat; inspection through the Nomarski microscope shows the surface contains a significantly large fraction of defects. The contrast seen in the optical image in Fig. 16 results from voids in the film likely resulting from the coalescence of InAs islands during growth. Meanwhile, both optical images of both the GaAs and the InGaAs appear smooth and show no significant microscopic defects at these growth conditions. The films in Fig. 16 were grown at 480ºC in order to stay at a temperature below where the stability of the InP might become an issue. Despite the low temperature, the optical images show there is no significant coverage of the SiO_2 surfaces at these growth conditions for InAs, GaAs, and InGaAs.

Further evidence for the confined growth of these materials to the exposed InP surfaces is shown in hole-patterned surfaces shown in the optical images in Fig. 17. The majority of the material is seen to grow out of the exposed InP, while limited material is seen deposited on the SiO_2 masked regions. The nominal growth thickness for the posts was 100nm (as measured on unmasked surfaces) and the oxide mask is nominally 60nm in thickness. The images show post structures extending out of the unmasked regions with approximately the same distribution in height regardless of the separation distance suggesting that the In and Ga on the SiO_2 is simply not sticking rather than moving laterally to the edges of the unexposed regions. The result is that these temperatures for InGaAs growth may be appropriate for the initial stages of nucleating in the exposed InP regions and supporting vertical growth out of the masked regions.

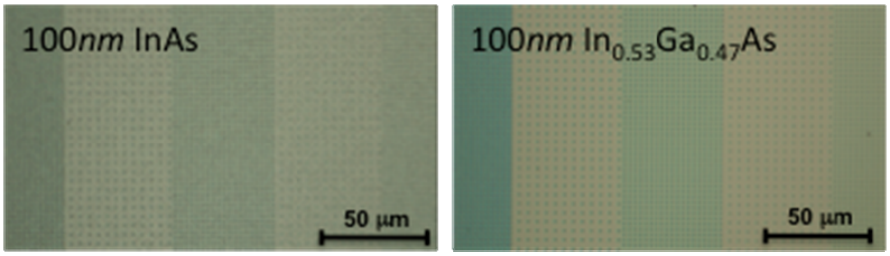

Fig. 17 Optical images of hole patterns in the SiO2 hard mask on the InP(100) surface for 100nm thick InAs and InGaAs films grown by MBE at 480ºC.

The growth of III-V compound semiconductors on SiO_2 patterned surfaces by solid source MBE requires finding two growth windows. The first is a window where the mobility or sticking of the elements on the SiO_2 are sufficient to prevent growth on the hard mask, while still promoting growth on the clean InP surfaces. A second growth window is subsequently required to encourage overgrowth of the masked areas once the growth has extended above the height of the mask. This second window is more difficult and as a starting point we have begun to look at the growth of thick InGaAs films on these masked surfaces.

Fig. 18 shows RHEED and optical micrographs of masked InP surfaces following 1 μm of InGaAs growth by MBE at (a) 480ºC and (b) 400ºC. For both growths, the growth rate was held constant at 2 Å/sec. The 480ºC growth showed no change in the RHEED during growth as the pattern remained streaky throughout. The optical images showed limited evidence of growth on the masked regions while significant growth was found on the exposed InP regions. However, most of the growth appeared to remain normal to the surface with limited lateral growth detected as seen in the image in Fig. 18. Growth at 400ºC appears similar although RHEED shows some additional spots suggestive of 3D growth on parts of the patterned wafer. The higher magnification images show there is some overgrowth of the SiO_2, but also shows high defect densities at the edges of the patterned growth areas.

At these growth conditions, (Ga,In)As tends to grow in a layer by layer mode, and the vertical growth of the InGaAs surfaces in Fig. 18 are consistent with this growth mode. The thermal stability of the InP prevents high temperature depositions around 600ºC, which is typically needed to transition over to a step-flow growth regime. One obvious possibility other than increasing temperature is to significantly lower the arsenic overpressure to find a window for lateral step flow growth. Initial results have thus far been inconclusive.

The growth of antimonides as a possible means of inducing a lateral growth over the SiO_2 masks was also explored since the antimonides tend to grow via a step-flow growth at temperatures around 500ºC. Initial attempts to grow GaSb directly on the InP surface proved unsuccessful. Fig. 19 shows the results after 200nm direct deposition of GaSb on InP. The RHEED is nearly amorphous with some weak polycrystalline rings and 3D spots, while the optical images show an extremely rough surface morphology. Whether this is a problem with oxide removal under an antimony flux or a more fundamental nucleation problem on the InP surface is not clear, but repeated growths showed little improvement. An alternative approach has been to grow an arsenide seed layer followed by growth of an antimonide. The right half of Fig. 19 shows the RHEED and optical images following the growth of 100nm GaAs on patterned InP, followed by the growth of 100 nm of GaSb. The RHEED looks primarily streaky, although with some polycrystalline rings

originating from some of the masked regions. The RHEED does show a marked improvement over the patterns obtained from direct GaSb growths. Optical images of the surface also show that the patterned regions are still quite visible, but the contrast between the patterned and unpatterned regions is greatly reduced owing to partial coverage of the SiO_2. Additional work is still needed to adjust the group V fluxes and identify the proper transition thicknesses for the arsenides, but initial results from this growth approach suggest an alternative growth window via the antimonides exists for lateral growth.

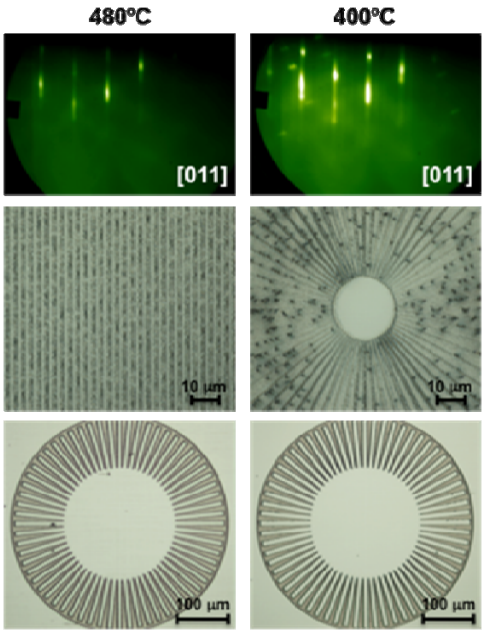

Fig. 18 RHEED and optical images of 1 µm thick InGaAs films grown by MBE at (a) 480ºC and (b) 400ºC.

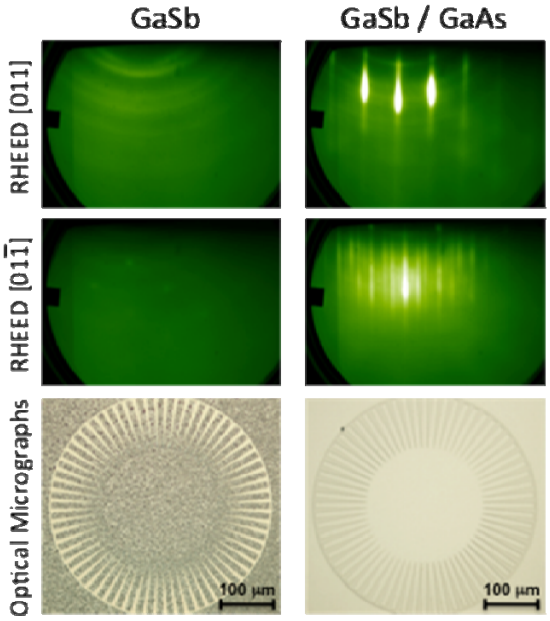

Fig. 19 RHEED and optical images of (a) 200 nm thick GaSb and (b) 100 nm GaSb / 100nm GaAs films grown by MBE at 480ºC on patterned InP(100).

2.6 Chemical Beam Epitaxy Growth System

CBE is ideally suited for the selective area growth needed for the InP growth initiation and subsequent epitaxial lateral overgrowth because of the chemical selectivity of the gas sources and the atomic layer control of a molecular beam system. During this program a system at UCSB that had been used to grow InGaAsP quantum well lasers as well as InP-based heterojunction bipolar transistors was to be brought up to working order specifically for epitaxial overgrowth. During this year significant work has been performed to prepare the CBE system for specimen growth, but equipment related set backs caused the operational timeline to be extended well beyond that proposed.

The CBE growth and preparation vacuum chambers, water cooling, gas lines, gas cabinets, exhaust and electronics cabinets were installed and are operational. The growth and preparation are all under vacuum. The group-V gas effusion cells have been modified to convert them from high-pressure (~700 Torr) injectors to low-pressure (~100 mTorr) injectors. This was done to improve safety and to make more efficient use of the source material. In addition to modification of the group-V gas cell injectors, the gas line valving and the addition of a turbo pump, the gas lines

themselves also had to be modified. Most of this has now been completed. Turbo pumps for the group III gas line and for the load lock required repair, however, despite being rebuilt, the pumps never managed to perform for more than a few weeks without requiring additional maintenance with the load lock pump eventually seizing.

The power, cooling water, compressed air, gaseous nitrogen facilities and two dedicated liquid nitrogen phase separators, one for the CBE growth chamber diffusion pump trap and one for the CBE growth chamber cryopanels, have been installed. The toxic gas monitor and some interlocks need to be installed.

Two CBE components were also found to require additional work. The group III gas injector source cell had a leak in one of the welds to the cell, was dismantled, cleaned, and welded properly. The growth manipulator heater was also non operational and required replacement and reassembly of the mounting plate. Laser-drilled orifices to limit the conductance of gases through the gas lines were installed; valving was tested as well as all source heaters. Gas cabinets and exhaust for the system were certified by university health and safety for operation.

Currently, the system is waiting for delivery and return of two turbo pumping units. The system unfortunately cannot be run without them. Once installed the system will undergo a final bake and the gas sources will be installed for operation allowing growths to once again resume on the system.

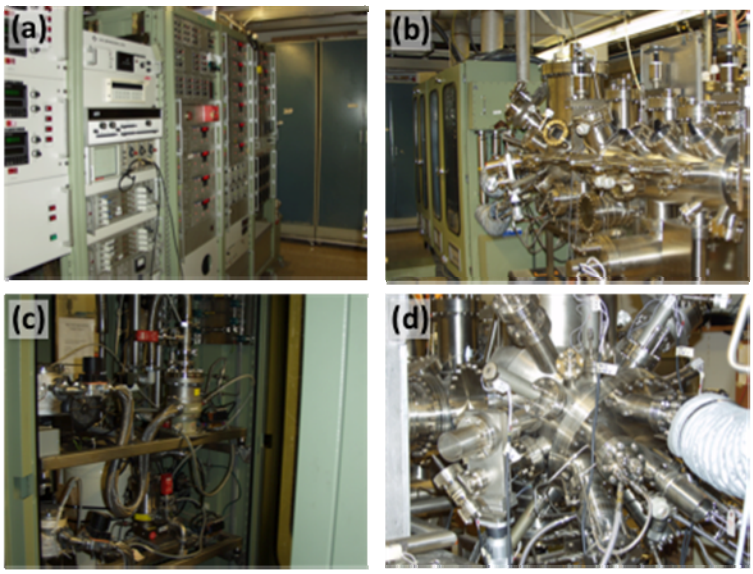

Fig. 20 Components of the CBE system brought on-line including; (a) electronics for pumping, source heating, and valve control, (b) the diffusion and ion pumps, which are now holding the growth and specimen preparation chambers under vacuum, (c) plumbing final utilities for gas line operation, and (d) installing the necessary gas lines from the source cabinets to the deposition chamber.

2.7 Summary

The fundamental nucleation and growth of As and Sb based III-V semiconductors on SiO_2 masked Si(100) and InP(100) surfaces were investigated via molecular beam epitaxy (MBE) to determine

the best growth windows for nucleation and lateral overgrowth. We determined surface preparation techniques for atomically clean Si surfaces for MBE and CBE growth by ex-situ etching of the surface SiO_2 by dilute HF and in-situ annealing. GaAs films on SiO_2 masked Si(100) surfaces showed preferential nucleation on the cleaned Si(100) surfaces with respect to the SiO_2 hard mask for growth between 450ºC and 650ºC. No significant coverage of SiO_2 surfaces at 450ºC growth conditions for InAs, GaAs, and InGaAs when nucleated on InP(100). Antimonides provide better lateral overgrowth than arsenides indicating transitions from layer-by-layer to step flow growth regimes in MBE may be critical for ELO. In future work using a CBE system, similar growth studies will be conducted.

2.8 Reference

1 S. M. Gates, R. R. Kunz, and C. M. Greenlief, "Silicon Hydride Etch Products from the Reaction of Atomic Hydrogen with Si(100)", Surf. Sci. 207, 364 (1989).

3. Publications

Julian, N., Mages, P.A., Zhang, C., Zhang, J., Kraemer, S., Stemmer, S., Denbaars, S., Coldren, L.A., Petroff, P., Bowers, J.E., "Coalescence of epitaxial lateral overgrown InP by MOCVD with v/iii ratio variation", submitted to Journal of Electronic Materials, 2011

Julian, N., Mages, P.A., Kraemer, S., Zhang, J., Stemmer, S., DenBaars, S. P., Coldren, L.A., Petroff, P., Bowers, J.E., "Coalescence phenomena in narrow-angle stripe epitaxial lateral overgrown InP by MOCVD", Electronic Materials Conference, 2011

Mages, P.A., Julian, N., Zhang, C., Coldren, L., DenBaars, S., Bowers, J.E., "Growth habit control of epitaxial lateral overgrown InP on Si substrates by MOCVD", Electronic Materials Conference, 2011